Oil & Gas Science and Technology – Rev. IFP Energies nouvelles, Vol. 67 (2012), No. 1, pp. 59-75

DOI: 10.2516/ogst/2011166

Dossier

Diagenesis - Fluid-Rocks Interactions
Diagenèse minérale - Équilibres fluides-roches

Late Dolomitization in Basinal Limestones of the Southern Apennines Fold and Thrust Belt (Italy)

A. Iannace[1], M. Gasparrini[2], T. Gabellone[1] and S. Mazzoli[1]

1 Dipartimento di Scienze della Terra, Università Federico II, Largo San Marcellino, 10, 80138, Napoli - Italy
2 IFP Energies nouvelles, 1-4 avenue de Bois-Préau, 92852 Rueil-Malmaison Cedex - France
e-mail: aleianna@unina.it - marta.gasparrini@ifpen.fr - tatyana.gabellone@unina.it - smazzoli@unina.it

Résumé — Dolomitisation tardo-diagénétique dans les calcaires de bassins triassiques de l'Apennin Méridional (Italie) — Les carbonates pélagiques triassiques de l'Unité de Lagonegro, dans l'Apennin méridional hébergent des corps dolomitiques discordants. Ces dolomies montrent les structures typiques connues comme "zébra" ou dolomite "à selle". Dans cette note, on présente les résultats d'observations de terrains et pétrographiques et les données géochimiques obtenues sur trois affleurements.

Les données de terrain indiquent que les structures de type "zébra" et bréchifiées sont contrôlées par la stratification très régulière des calcaires micritiques. La dolomitisation a comporté le remplacement du calcaire et de la précipitation de dolomite cristalline dans les vides sous un champ de contraintes extensionnelles.

Les températures d'homogénéisation sont comprises entre 80 et 120 °C, avec un mode à (95 ± 10) °C. Après une correction de pression, elles indiquent une température maximale de formation de la dolomie d'environ 110-115 °C. Les températures de fusion de la glace indiquent une salinité comprise entre 2 et 6 wt% NaCl eq, avec une moyenne de 4.2 %. Les valeurs de $\delta^{13}C$ sont comparables à celles de l'eau de mer triassique, tandis que les valeurs de $\delta^{18}O$ sont fortement appauvries. Les valeurs du rapport $^{87}Sr/^{86}Sr$ sont au contraire plus élevées que celles estimées pour l'eau de mer triassique, mais comparables à celles du Miocène Moyen-Supérieur.

Ces résultats indiquent une dolomitisation accomplie par des fluides relativement chauds avec une salinité voisine de celle de la mer et une composition isotopique comprise entre celle de l'eau de mer et celle de saumures de bassin. On propose que cette dolomitisation a été achevée par les eaux expulsées par les formations qui entourent les carbonates pélagiques triassiques ou celles du mélange sous-jacent. L'intégration des données sur l'histoire thermique et de la déformation indique, si l'on assume un équilibre thermique avec les roches encaissantes, que ce phénomène ait eu lieu après le pic d'enfouissement pendant les premiers stades de l'exhumation. Enfin, puisque les dolomies sont assez répandues dans la région, il est bien possible qu'une importante circulation de fluides ait intéressé l'entier *fold- and thrust-belt* pendant la déformation, y compris les unités de la Plate-forme Apulienne, qui héberge des importants réservoirs d'hydrocarbures.

Abstract — Late Dolomitization in Basinal Limestones of the Southern Apennines Fold and Thrust Belt (Italy) — *The Triassic pelagic carbonates of the Lagonegro Units from the southern Apennines fold and thrust belt host discordant bodies of dolostone. These rocks show textural features typical of zebra or saddle dolomites. In this contribution, the results of field observations, petrography and geochemical analyzes performed on samples from three different outcrops are presented.*

Field data indicate that the peculiar zebra-type rock and brecciated fabrics were controlled by regular bedding of the micritic, pelagic limestones. The dolomitization resulted in the replacement of the host limestones and subsequent void-filling precipitation of dolomite in a dilatational stress field.

Homogenization temperatures (Th) are in the range 80 - 120°C, with a clear mode of 95 ± 10°C. When corrected for maximum pressure, they indicate an upper limit for dolomite formation around 110 - 115°C. Melting temperatures of ice (Tm_i) point to salinities in the range 2-6 wt% NaCl eq, with a mean of 4.2%. $\delta^{13}C$ values overlap those of the Upper Triassic seawater, whereas the $\delta^{18}O$ values are significantly depleted compared to the coeval seawater. $^{87}Sr/^{86}Sr$ values are higher with respect to Upper Triassic seawater, and partially overlap Middle-Upper Miocene values.

The performed analyzes indicate a dolomitization process driven by warm fluids (110 - 115°C) with a salinity close to that of seawater and O-isotope ratios comprised between seawater and formation waters. It is suggested that the dolomitization was accomplished by formation waters squeezed out or from surrounding lithologies or from the underlying mélange *units. Integration with available thermal data on the collisional history of the belt suggests that the fluid-flow took place after maximum burial, in the early stages of exhumation, in the assumption of a fluid in thermal equilibrium with the host rocks.*

According to literature data, the dolomitization event was quite widespread. It can be argued that it was part of a major fluid-flux associated with fold and thrust belt development, which possibly affected the Apulian Platform carbonates located in the foreland. The latter, now buried below the nappe stack, hosts some of the major oil fields of continental Europe.

INTRODUCTION

Dolomitization is a replacement process requiring a large amount of Mg-rich fluids interacting with a limestone precursor. It is now generally accepted that several mechanisms can be responsible for such a rock-water interaction. These mechanisms may occur at different stages in the diagenetic evolution of carbonate rocks, ranging from processes acting soon after deposition to late-stage, epigenetic processes operating well after lithification and exhumation (Warren, 2000; Machel, 2004). Among the late-stage models of dolomitization, replacement by warm to hot solutions in the frontal parts of orogenic belts has been increasingly recognized in recent years (Qing and Mountjoy, 1994; Boni *et al*., 2000a; Swennen *et al*., 2003; Gasparrini *et al*., 2006a). Originally, this model was introduced to explain the peculiar vuggy dolomites, often displaying zebra textures and saddle-shaped crystals, associated with many MVT-type mineralizations of North America (Jackson and Beales, 1967; Anderson and Macqueen, 1982; Machel *et al*., 1996). It is presently debated whether the large scale circulation of fluids is triggered by tectonic charge or by the hydraulic head induced by regional topography (Garven and Freeze, 1984; Oliver, 1986; Bethke and Marshak, 1990; Deming and Nunn, 1991; Ge and Garven, 1994; Morrow, 1998). Whatever the origin of the fluid-flow, the dolostone bodies are generally found in the undeformed foreland at the front of the fold and thrust belt and may be associated with deep-seated, sub-vertical normal faults (Taylor and Sibley, 1986; Hurley and Budros, 1990; Berger and Davies, 1999; Wendte *et al*., 2009; Lavoie and Chi, 2010; Shah *et al*., 2010), although several examples of dolomites formed within the fold and thrust belts itself also exist (Qing and Mountjoy, 1994; Swennen *et al*., 2003; Vandeginste *et al*., 2005).

This paper illustrates a case study of dolomitization of Triassic basinal limestones within a Neogene fold and thrust belt (southern Apennines, Italy). The paper is based on the analysis of a few outcrops, described in the late 60's by Scandone (1967). Nevertheless, no specific research was carried out to unravel the origin and timing of the dolomitic rocks described by this author. This study presents petrographic, geochemical and fluid inclusions data that, together with field evidences, strongly suggest that the dolostone bodies were formed during or after the Neogene regional tectonic shortening, due to the actions of overpressured warm fluids. A more comprehensive regional study of all the dolomitized bodies of the same tectonic unit, both in outcrop and in the subsurface, is presently in progress in order to better define the relationships of the fluid-flow and the structural history of the tectonic belt.

1 GEOLOGICAL SETTING

The southern Apennines fold and thrust belt consists of a stack of several tectonic units made of Mesozoic-Paleogene successions and their flysch-like Neogene cover, tectonically superposed onto the buried part of the Apulian Platform shallow-water carbonates (Mostardini and Merlini, 1986; Casero *et al*., 1988; Cello and Mazzoli, 1998). This complex fold and thrust belt mainly formed as a result of Neogene deformation of the former Adriatic passive margin during Europe-Africa plate collision (Mazzoli and Helman, 1994, and references therein).

From top to bottom, the belt consists of ocean-derived units, shallow-water carbonates of the Apennine Platform Units and pelagic and hemipelagic basinal sediments of the Lagonegro Units. The lowermost part of the Lagonegro

Basin succession consists of the *Monte Facito* Formation, given by Lower-Middle Triassic shelfal, fine-grained siliciclastics containing carbonate buildups with dasycladacean algae and sponges (Scandone, 1967; Ciarapica *et al*., 1990). The overlying *Calcari con Selce* Formation, Upper Triassic in age, consists mainly of micritic limestones containing thin-shelled bivalves and radiolarians, with beds and nodules of chert. Locally they consist of calcarenites, calcirudites and marls. According to Scandone (1967) the *Calcari con Selce* Formation is actually represented by dolostones in many outcrops from the northern area of the Lagonegro Basin (from Salerno to Val d'Agri), particularly in the hanging wall of a major thrust within the Lagonegro Units. Conversely, no dolostone occurrence is reported in the Lagonegro Basin cropping out further to the south *(Fig. 1)*. The *Scisti Silicei*, *Galestri* and *Flysch Rosso* formations represent the truly deep-water stage of the basin. The term "flysch" is inherited from old literature, since the latter formation actually represents pre-orogenetic sediments. True siliciclastic, turbidite deposits of the compressional stage are represented by the overlying Miocene sandstones and shales.

The deformation history of the Lagonegro Units was outlined by Scandone (1972). A more detailed structural study was performed by Mazzoli *et al*. (2001 and references therein), who proposed a different structural evolution. From Triassic to Cretaceous times, the southern Apennines were in a passive margin phase *(Fig. 2a)*. Shortening started during the Miocene, with a first phase of buckling and minor thrusting that caused the "closure" of the Lagonegro Basin *(Fig. 2b)*. In Pliocene times, a second phase of thrusting led to the regional duplication of the Lagonegro Units *(Fig. 2c)*. This was followed by the emplacement of the allochthonous wedge

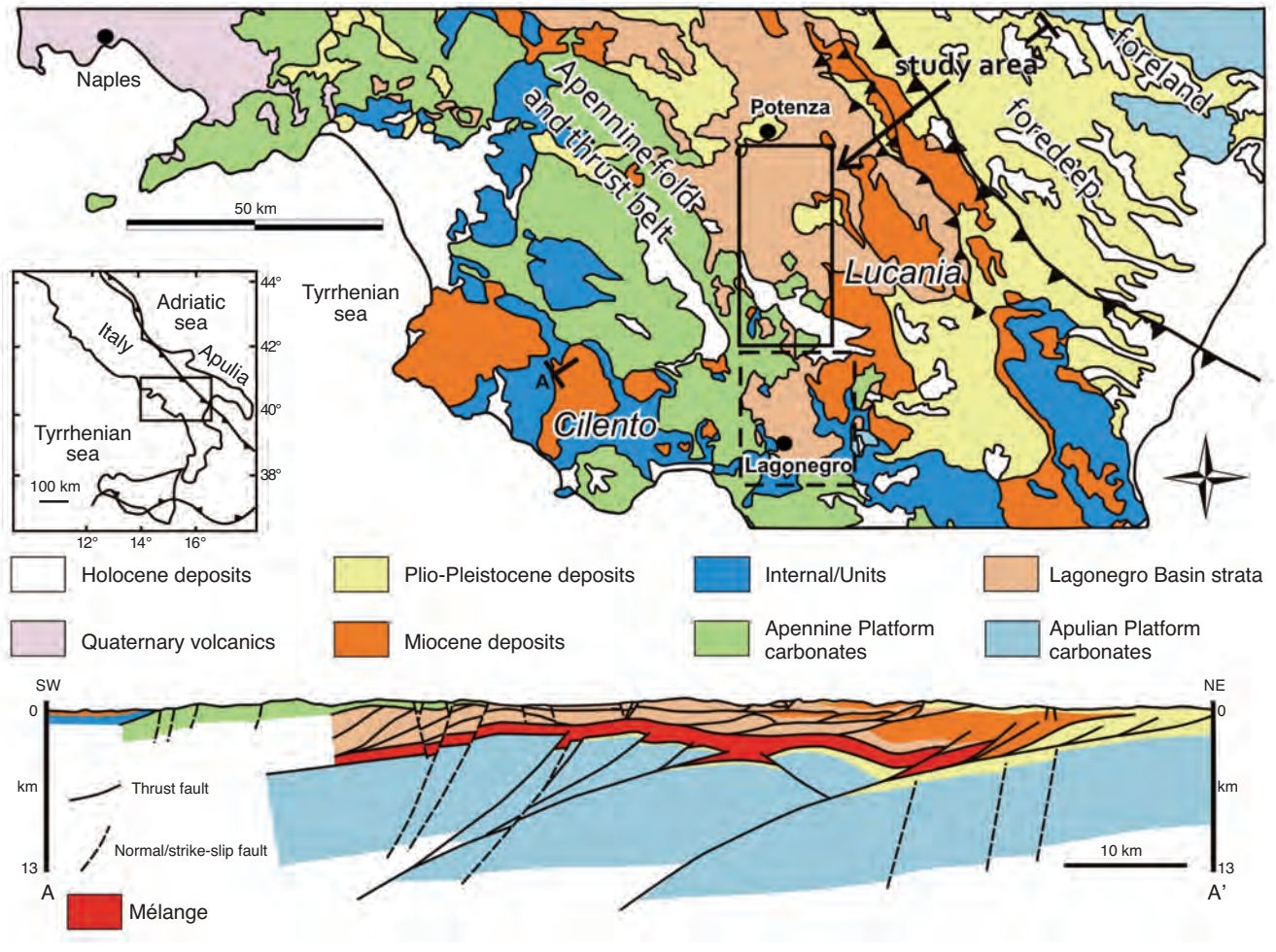

Figure 1

Simplified geological map and cross section of the southern Apennines (modified after Mazzoli *et al*., 2008). The study area is located in the frame bordered by continuous line. The southern Lagonegro Basin area, where no dolostones crop out, is enclosed in the frame with dashed line.

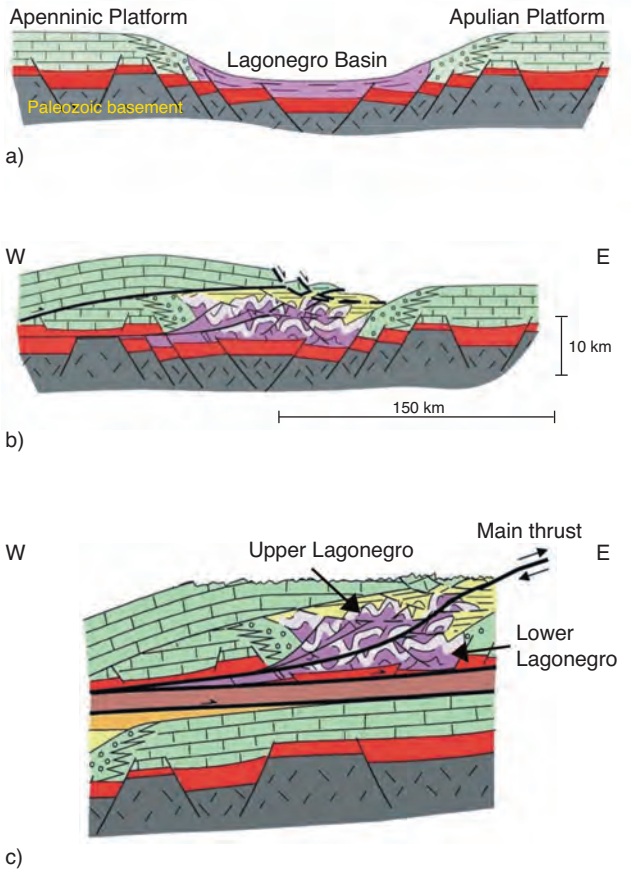

Figure 2

Summary structural model for the evolution of the southern Apennines from the Triassic to the Plio-Pleistocene (modified after Shiner *et al*., 2004). Three different phases of structural evolution are illustrated: a) Mesozoic-Paleogene passive margin phase; b) Miocene buckling and first thrusting phase in the Lagonegro basin; c) Pliocene second phase of thrusting that led to the doubling of the Lagonegro Units.

above the westernmost portion of the Apulian Platform, a process which formed the structural traps hosting the major oil fields of southern Italy (Shiner *et al*., 2004). Gravitational readjustments dominated within the allochthonous wedge, triggering denudation and tectonic exhumation (assisted by erosion; Mazzoli *et al*., 2008). Active shortening was taken up by the underlying Apulian crust, producing basement-involved inversion at depth.

The burial history of the succession was constrained by recent studies based on thermal and thermochronological data from the northern Lagonegro Basin (Aldega *et al*., 2003, 2005; Corrado *et al*., 2005; Mazzoli *et al*., 2008) which indicate a maximum burial of 3.8 km and a temperature peak in the range of 130-160°C, reached in the Miocene during the first thrusting phase. The second phase of thrusting was accompanied by exhumation. The latter is well constrained by apatite fission track data that provide cooling ages clustering around 5.5 Ma (Mazzoli *et al*., 2008). To the south (Monte Sirino area) maximum reconstructed burial is in excess of 5 km and peak temperatures are above 180°C, while exhumation is substantially younger, apatite fission track cooling ages clustering in the last 2.5 Ma (Corrado *et al*., 2002; Mazzoli *et al*., 2008).

2 MATERIALS AND METHODS

The studied succession consists in the upper part of the *Calcari con Selce* Formation, close to the boundary with the overlying *Scisti Silicei* Formation. The main investigated sites are located in the surrounding area of Pignola village, south of Potenza, and more precisely along the road connecting Pignola to Abriola between km 10.9 and km 11.4 (1 in *Fig. 3*) and within an abandoned quarry front along the same road (2 in *Fig. 3*). These sites were well illustrated by Scandone (1967) who observed that within the *Calcari con Selce* Formation, dolostone bodies cut across the bedding and in some cases the boundary between the two lithologies is represented by fractures. A third investigated site was located further to the south close to Mount Manca di Vespe (3 *in Fig. 3*).

A total of 40 rock specimens of both dolostones and precursor limestones were sampled within the *Calcari con Selce* Formation from the three investigated sites which will be referred as 1) road, 2) quarry and 3) Mount Manca di Vespe *(see Fig. 3)*. Polished slabs were prepared and stained with Alizarin red-S. About 30 thin sections (30 to 35 mm thick) were prepared for conventional and cathodoluminescence (CL) microscopy. From the coarser crystalline samples, double-polished thick sections (100-120 μm thick) were prepared for Fluid Inclusion (FI) petrography and microthermometry. UV-light microscopy was used to characterize the fluid system (aqueous *versus* hydrocarbon) of FIs in the different mineral phases with a 100W Mercury vapor lamp associated to an polarized microscope.

Conventional and cathodoluminescence (CL) microscopy was accomplished on all thin sections at IFP Energies nouvelles (France). Thin sections were studied by the use of a Nikon LV100 Eclipse POL. The device used for cold CL is a Technosyn 8200 Mark II (OPEA, France).

Dolomite stoichiometry was calculated on 10 samples by means of diffractogram analyses, using the cell and Rietveld refinement method developed at IFP Energies nouvelles (Turpin *et al*., this volume). The samples were analyzed with an analytical X'pert PRO PW 3040/60.

Powders from the different carbonate phases were obtained by drilling the rock slabs using a dental drill. Analyses to determine the O, C and Sr isotope ratios were performed at the *Institute für Geologie, Mineralogie und Geophysik* of Ruhr-University (Germany). Oxygen and carbon isotope

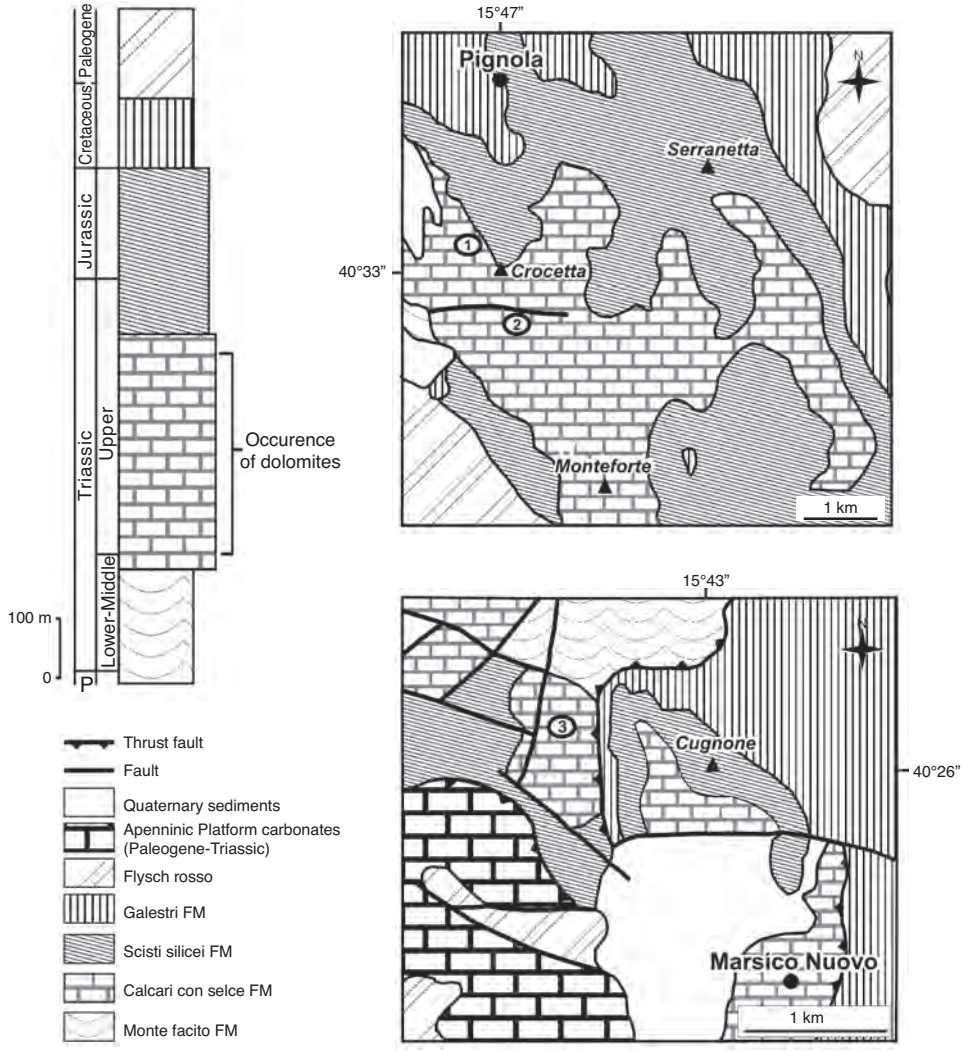

Figure 3

Simplified stratigraphic column and simplified geological maps of the study area. Numbered spots indicate the location of the sampled sites: 1) road; 2) quarry; 3) Mount Manca di Vespe.

ratios were measured on the CO_2 produced after etching with orthophosphoric acid at 90°C with a Finningan Delta S spectrometer. The dolomite acid correction factors from Rosenbaum and Sheppard (1986) were applied. Measurements of Sr isotope ratios were carried out on 1 mg of powder in a 2.5 M HCl. The $^{87}Sr/^{86}Sr$ was determined by means of a Thermal-ionization Finningan Mat 262 Mass Spectrometer. The Sr isotope ratios were then normalized to a ratio value of $^{87}Sr/^{86}Sr = 0.1194$. The precision was better than 0.00004.

Fluid Inclusion (FI) microthermometry was carried out with a Linkam MDS 600 heating-freezing stage, calibrated with synthetic FIs, and mounted on a Nikon LV100 Eclipse associated to a 100 W Mercury vapor lamp (IFP Energies nouvelles). The Linksys 32 software enabled all the operations for FI microthermometry. The software package FLUIDS (Bakker, 2003, 2009) was used to further characterize the fluids from the FI study. AQSO1 was used to calculate salinities from final melting of ice (Tm_i) in the binary H_2O-NaCl system (Bodnar, 1993). The application BULK allowed to calculate bulk fluid properties (*e.g.* density) of individual FIs using the equation of state for aqueous systems of Krumgalz *et al*. (1996) and the volume fractions of the liquid phase of FIs at room temperature. The program LONER32 was used to calculate the isochore slope for FIs from the different phases according to the model of Bodnar and Vityk (1994).

3 FIELD OBSERVATIONS

The *Calcari con Selce* Formation in the investigated sites consists of dark grey, well bedded (5 to 20 cm) mudstone to wackestone containing sub-rounded, cm-sized chert nodules as well as chert lenses, up to 15 cm thick showing good lateral continuity (up to several meters). The limestone beds are generally confined by thin marly interlayers. At Pignola, the limestones host calcite nodules (a local replacement of the chert), 1 to 8 cm in diameter.

The macroscopic features of the dolostone bodies are well exposed in the quarry outcrop. The dolostone forms irregular bodies within the well-bedded limestones of the *Calcari con Selce* Formation. The boundaries between the two lithologies are sharp and cut through the bedding planes *(Fig. 4)*. Tongues of unreplaced limestone are however present between dolomitized beds. This shows that the marly, less permeable interlayers which occur within the limestones, possibly exerted a control in focussing the dolomitizing fluids.

Chert lenses may be still preserved within the carbonates that were affected by dolomitization. On the contrary, the calcite nodules, which formerly replaced the chert, were completely dolomitized.

Two main dolomite types are recognised in the field:

– a dark to light grey dolomite type, of purely replacive origin as indicated by the preservation of some sedimentary features of the precursor carbonate, such as plane-parallel and convolute laminations and ghosts of radiolarians and thin-shelled bivalves, and;
– a milky white and void-filling one.

These two dolomite types may form alternating dark grey and white bands *(Fig. 5a)* resembling to what in literature is reported as zebra-dolomites (Beales and Hardy, 1980; Fontboté and Amstutz, 1983; Arne and Kissin, 1989; Nielsen *et al*., 1998). These roughly bed-parallel bands are frequently confined by fractures (the *fratture-diaframma* described by

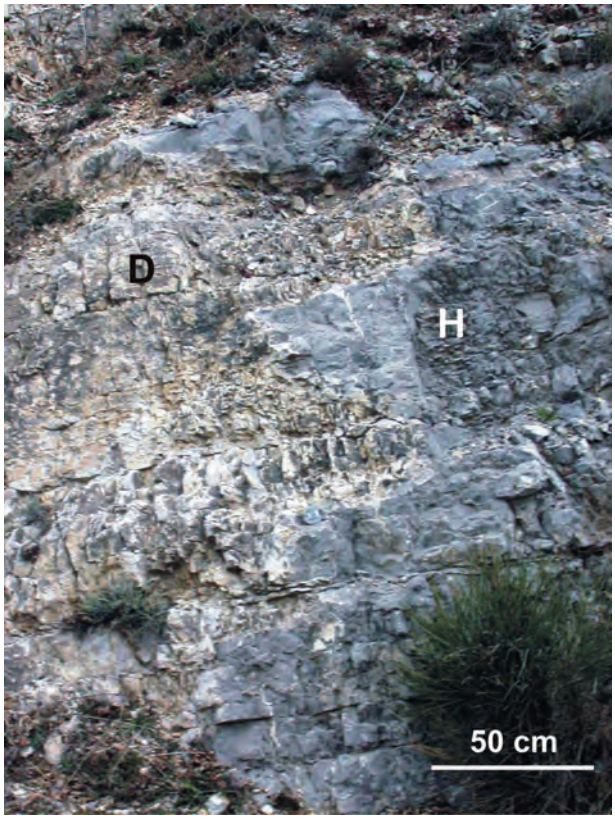

Figure 4

Contact between host limestone (H) and dolostone (D). The boundary between the two lithologies is sharp and cut through the bedding planes.

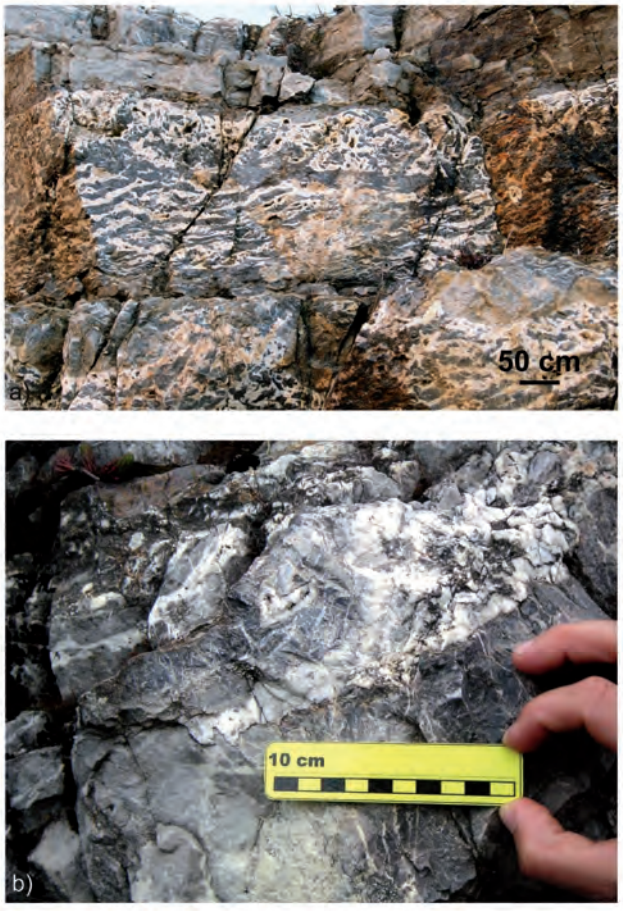

Figure 5

Field photographs of the late dolomites of the Lagonegro Basin. a) Zebra structures. The white dolomite is very abundant, the proportion between the grey dolomite and milky white dolomites is about 1:1. b) Grey replacive dolomite and white-sparry dolomite cements. The boundary grey-white dolomite locally correspond with a bedding-parallel stylolite associated to a thin film of insoluble residue.

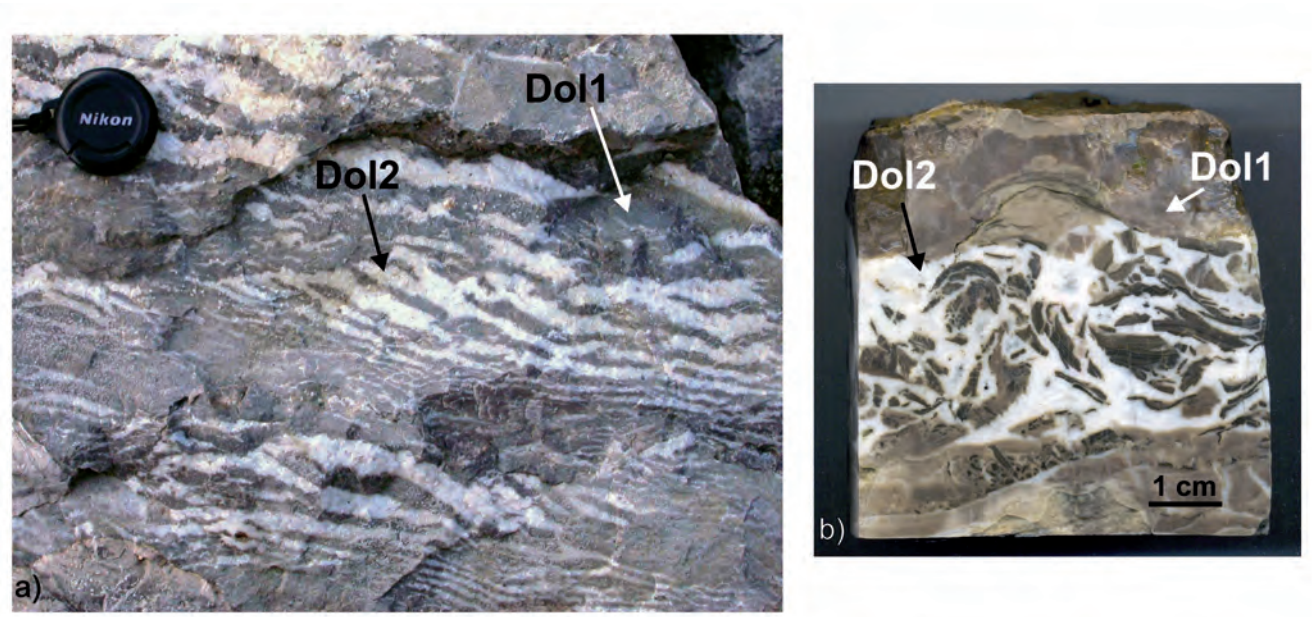

Figure 6

Late dolomites of the Lagonegro Basin. a) Zebra structures with a shear component. b) Polished hand specimen of hydraulic dolomitic breccias.

Scandone, 1967). The zebra-like structures are not ubiquitous and seem to be confined in some layers of the succession, comprised between layers composed of replacive grey dolomite only. It was observed that, where the carbonates are thicker bedded, the grey replacive dolomite is dominant and the zebra-structures tend to be absent, whereas in thinner beds bedding parallel stylolites are better developed and concentrated in the grey replacive portion, and zebra-structures tend to be more abundant. In the latter case, the proportion between the grey dolomite and milky white dolomites is about 1:1, *i.e.* the white, void-filling dolomite is very abundant *(Fig. 5a)*. Locally stylolites associated to a thin film of insoluble residue constitute the boundaries between grey and white dolomite bands *(Fig. 5b)*.

Locally, bands of void-filling dolomite are oriented obliquely with respect to the main, bed-parallel zebra *(Fig. 6a)*. This *en echelon* vein array geometry is consistent with a simple shear component of the deformation controlling vein development (Mazzoli and Di Bucci, 2003; Mazzoli *et al*., 2004, and references therein), a feature that has been frequently described in other zebra-dolomites (Wallace *et al*., 1994; Nielsen *et al*., 1998; Vandeginste *et al*., 2005; Diehl *et al*., 2010). Bedding-parallel simple shear may be related with flexural slip/flow folding, or be associated with the gliding of rock panels during thrusting.

Brecciated facies are also frequent *(Fig. 6b)*. They consist of cm- to dm-large clasts of grey replacive dolomites engulfed by white dolomite cements. The clasts display a sharp boundary and are generally broadly rectangular in shape, although smoothened to curved surfaces are also observed. Evidence of dissolution was locally observed at the borders of the grey dolomite clasts.

Dolomitization appears to post-date the development of a spaced, pressure-solution cleavage that occurs in the precursor limestone and is preserved with the same geometric pattern in dolomitized portions of the succession. This cleavage, according to Mazzoli *et al*. (2001), developed during the first compression phase *(Fig. 2b)*.

A set of calcite veins, perpendicular to bedding, sometimes in *en echelon* arrays, may be locally present in the unreplaced limestone close to the dolomitization front. Within the dolomitized bodies, similar veins are instead filled with dolomite. All these vein systems probably belong to the *en echelon* arrays of veins, described by Mazzoli and Di Bucci (2003) and Mazzoli *et al*. (2004), and interpreted as a result of NW-SE oriented, minor horizontal extension post-dating early buckling and associated layer-parallel shortening. The replacement of these veins by dolomites would suggest again that dolomitization post-dated the early phases of deformation.

The studied dolostone bodies were affected by post-dolomitization extensional tectonics, since steep, normal faults cut through the different dolomite types and display no geometrical relationship with the dolomitization fronts.

4 PETROGRAPHY

In the study area, the carbonates of the *Calcari con Selce* Formation consist of mud- to wackestone containing radiolarians and very thin bivalves, commonly recrystallized. These limestones show a uniform dull orange CL. They are cross-cut by veins (up to 150 mm in thickness) filled with dull orange to non-luminescent calcite *(Fig. 7a, b)*. The trace of these calcite veins stops at the contact with the calcite nodules (possibly replacing some of the sedimentary chert nodules), that on the contrary, consist of blocky crystals with a bright orange CL colour *(Fig.7a-d)*. The transition from limestone to calcite filling the nodules frequently consists of euhedral rhombs of dolomite (planar-E texture), 50 to 250 μm in diameter and with bright red CL, which replace the limestone micrite, as well as the calcite in the veins *(Fig. 7a-d)*. These diagenetic phases pre-date the development of the large dolomitized bodies which are the main focus of this study.

Three different types of dolomites have been distinguished according to petrography within the dolostone bodies of interest. They were called respectively Dol1, Dol2 and Dol3. Dol1 is volumetrically the most abundant and corresponds to the grey dolomite observed in outcrops and hand specimens. It consists of a non-planar-A mosaic of cloudy dolomite crystals 10 to 60 μm in diameter, showing straight extinction and dull red, uniform and unzoned CL *(Fig.7e, f)*.

Dol2 is a less abundant though ubiquitous phase in dolomitized outcrops. It corresponds to most of the white dolomite recognised in the field. The contacts between Dol1 and Dol2 are not transitional and correspond to an abrupt increase in crystal size *(Fig. 7e, 8a)*. Dol2 crystals may range from 800 μm up to several mm in size. They show a non-planar-A texture and are commonly elongated with main length parallel to the growth direction (*i.e.* towards the cavity centre; *Fig. 8a*). They show a strong sweeping extinction, curved crystal faces and cleavage planes, typical of saddle dolomite *(Fig. 8b)*. Dol2 crystals commonly display cleavage twins which may be curved as well. The Dol2 crystals are uniformly cloudy indicating the presence of inclusions homogeneously distributed within the crystals and have a dull red and uniform CL undistinguishable from the one of Dol1 *(Fig. 7f)*. The last crystal generation of Dol2, *i.e.* the one closer to the cavity centre, shows a non-planar-C texture *(Fig. 8c)*. These latter crystals display a scimitar-like shape and may exhibit a more or less developed zoning due to the alternation of zones with different FIs content. Typically, the last growth zone of the Dol2 crystals shows a dull orange CL *(Fig. 8d)*.

Dol2 is either the last dolomite phase which lines vuggy pores and fractures or, in other cases, it is followed by Dol3. Locally, the pores comprised between Dol2 crystals growing in opposite directions of a cavity, are filled by a micro-breccia in which angular clasts of Dol2 (100-400 μm in diameter) are merged within a finer dolomite matrix. More commonly the clasts of Dol2 are cemented by the later Dol3 *(Fig. 8e, f)*. The presence of these microbreccias indicates that the dolomites were affected by deformation after their emplacement.

Dol3 is not always present in the analyzed samples. It post-dates the white dolomite and is macroscopically recognisable in hand specimens as it shows a translucent appearance. It is composed by clear crystals of dolomite, locally showing non-planar-C texture and growing in crystallographic continuity with Dol2. In the latter case the crystals can be up to several mm in diameter. More commonly, Dol3 crystals fill thin fractures which cut through Dol1 and Dol2 *(Fig. 8c, d)* and no crystallographic continuity is observed. Dol3 crystals show no zonations and are dark red under CL up to non-luminescent *(Fig. 8d-f)*. This phase is also found in micro-brecciated dolomite samples cementing the angular clasts of Dol2 *(Fig. 8 e, f)*.

5 FLUID INCLUSIONS

The study of fluid inclusions (FIs) was accomplished on dolomite cements from the three sampled localities.

One sample containing a calcite nodule pre-dating the dolomites was investigated as well. The calcite contains 2-phase liquid-rich FIs which showed a behaviour suggesting that they underwent thermal reequilibration and leakage. Indeed, the recorded homogenization temperatures (*Th*) cover a large range of values and the homogenization measurements repeated on the same FI commonly resulted in increasing recorded temperatures. These results of microthermometry were therefore not worth to be graphically presented.

Dol1 contains abundant primary FIs, but their small size (< 2 μm) hindered any further characterization.

Dol2 and Dol3 contain FIs of primary origin, which are concentrated within crystal cores or are distributed along growth zones. They are 2-phase liquid-rich (degree of fill above 0.9), irregular to crystallographically controlled (*i.e.* one or more sides of the FI parallel crystal borders or cleavage planes) and up to 7 μm in length. UV-light microscopy suggested the aqueous nature of the fluids. Homogenization (*Th*) occurred in the liquid field. The nucleation of ice-like phases occurs between – 35 and – 48°C during the first cooling run. More than half of the FIs are characterized by metastability of the final melting of ice (Tm_i). In these FIs, the ice melts suddenly at temperatures above those derived from thermodynamic criteria. These melting temperatures, which may occur well above 0°C, have no meaning in terms of fluid salinity (Goldstein and Reynolds, 1994). Only the results from FIs showing an unambiguous stable behaviour have been considered.

The main results of FI microthermometry are summarized in Figure 9a, b. Dol2 and Dol3 cements from the three

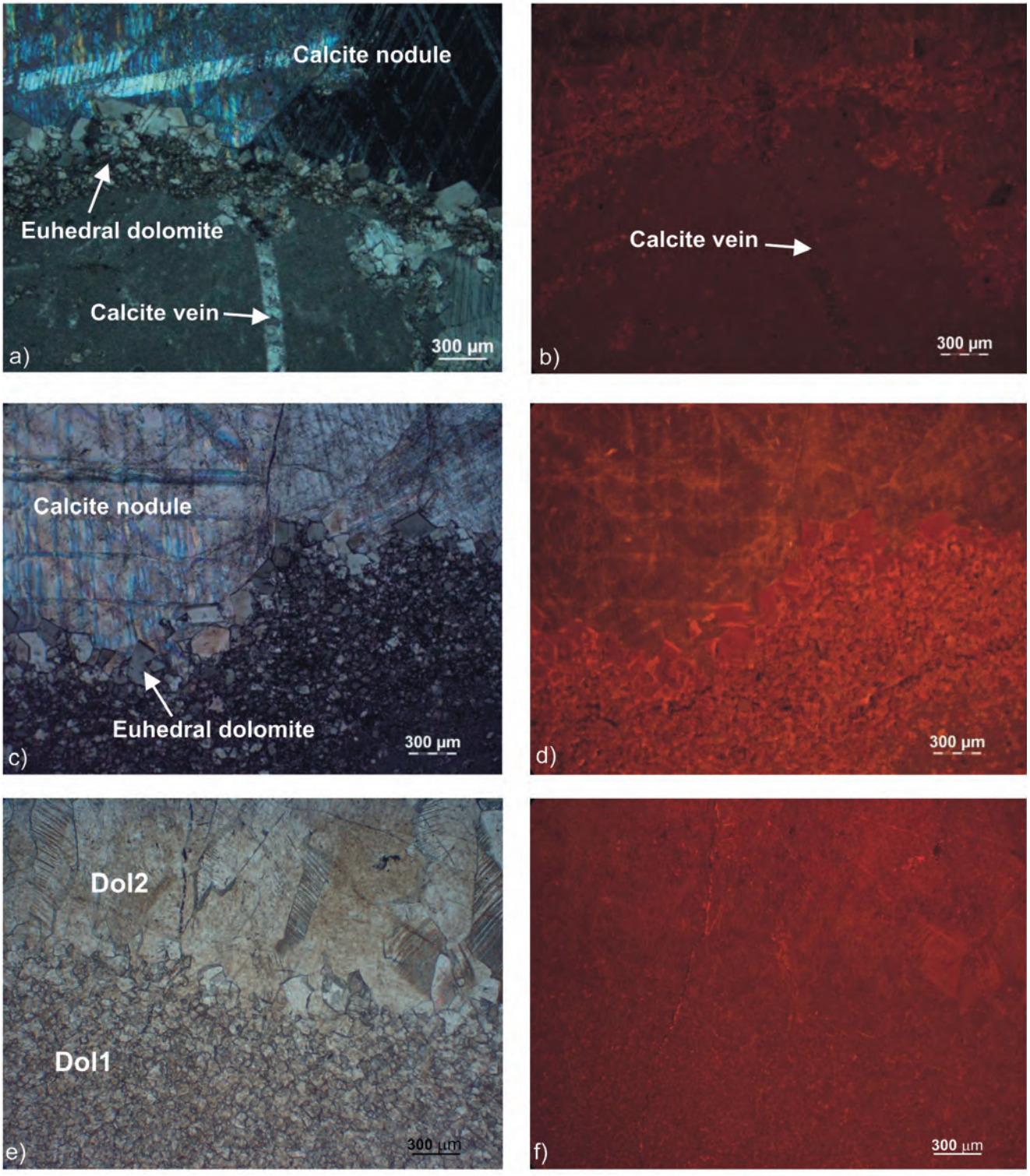

Figure 7

Photomicrographs. Scale bar is 300 µm. a) Dolomite host rock (mudstone) cross-cut by a calcite vein that stops at the contact with a calcite nodule. The latter is bordered by euhedral rhombs of dolomite. Cross-polarized light; b) CL image of a). The mudstone shows an uniform dull orange luminescence, whereas the calcite vein is non luminescent; c) Calcite nodule bordered by euhedral rhombs of dolomite. Plane-polarized light; d) CL image of c). The calcite nodule is bright orange, whereas the euhedral dolomite shows bright red luminescence; e) Dol1 and Dol2 showing non transitional contact. Plane-polarized light; f) CL image of e) showing Dol1 and Dol2 with undistinguishable dull red and uniform luminescence.

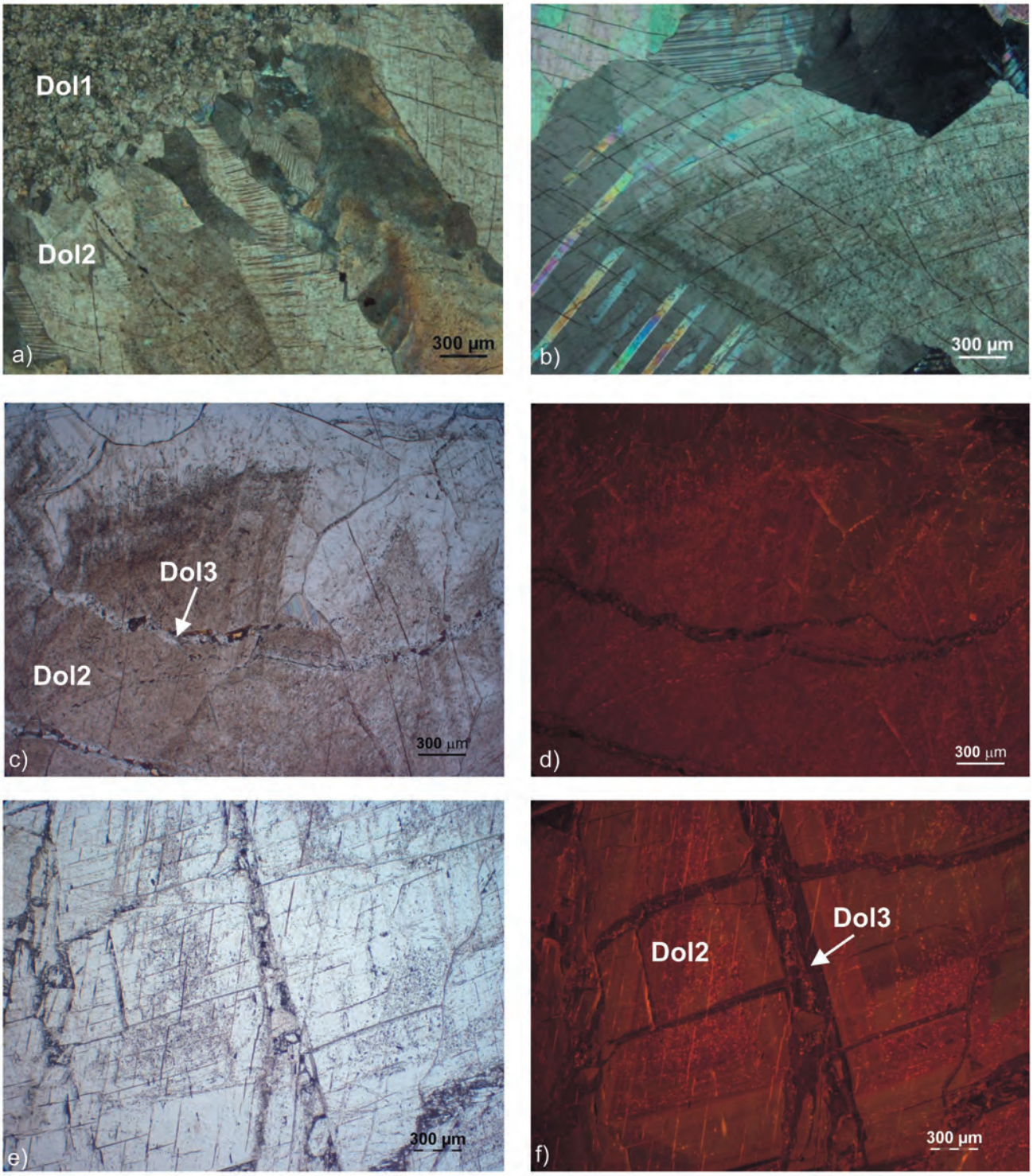

Figure 8

Photomicrographs. Scale bar is 300 µm. a) Abrupt transition from Dol1 to Dol2. Dol2 crystals are elongated towards the cavity centre and twinned. Cross-polarized light; b) Particular of a Dol2 crystal displaying curved crystal twins and curved cleavage. Cross-polarized light; c) Dol2 given by curved crystals, uniformly cloudy. Dol3 is present in the vein that cross-cut Dol2 crystals. Plane light photomicrograph; d) CL image of c). The last growth zone of the Dol2 shows a dull orange CL, whereas Dol3 is non-luminescent; e) Micro-brecciated dolomite in which angular clasts of Dol2 are cemented by Dol3. Plane-polarized light; f) CL image of e). Dol2 presents a dull red CL with the last growth zone showing orange CL. Dol3 is non-luminescent.

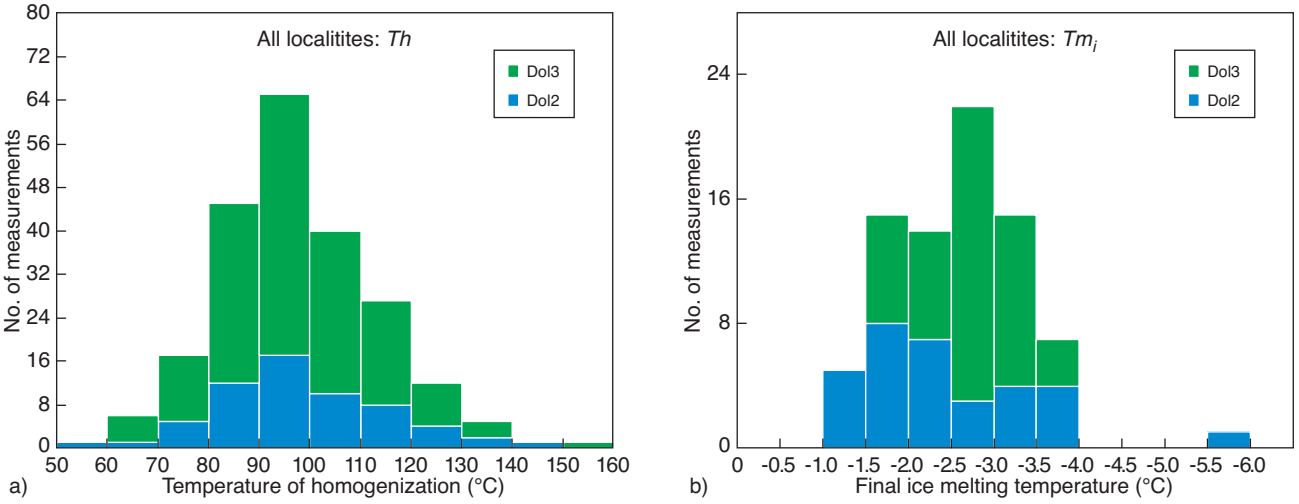

Figure 9

Histograms showing FIs data distribution in Dol2 and Dol3 cements from all localities. a) Homogenization temperature (*Th*) values. b) Ice melting temperature (Tm_i) values.

sampled localities show a very good overlap of both *Th* and Tm_i. Most *Th* values are in the range 80-120°C. This relatively large range of values could suggest thermal reequilibration of some FIs. Nevertheless, the frequency distribution of *Th* data is very symmetric and *Th* measured in FIs of the same assemblage are consistent. These evidences indicate that the *Th* variations are more possibly due to the FI distribution within the crystals (*e.g.* core *versus* external part, different growth zones; Goldstein and Reynolds, 1994). An overall *Th* mode at 95°C is established when considering the three localities together, with no differences between the FIs of the two dolomite cements *(Fig. 9a)*. In particular, a clear mode around 95°C can be recorded in the dolomite cements of the samples collected at the quarry and along the road (location 1 and 2 respectively in *Fig. 3*), whereas two modes are shown at 85°C and 110°C by the samples from the Mount Manca di Vespe outcrop (location 3 in *Fig. 3*), with the first mode being dominant. Most of the Tm_i values for FIs in both Dol2 and Dol3 fall in the range between –1 to –3°C, with main mode at –2.7°C. No differences were recorded from one locality to an other. These Tm_i values correspond to salinities (Bodnar, 1993) in the range 2-6 wt% NaCl eq *(Fig. 10)*, with mean value of 4.2%.

In conclusion, beside minor variations, it can be stated that Dol2 and Dol3 from the three sampled localities were precipitated in the burial environment from fluids having similar temperatures and salinities, which are in the range of slightly modified to normal marine seawater.

Calculations were accomplished in order to apply a geologically coherent pressure correction to the homogenization temperatures obtained from this study. Bulk densities were calculated for individual FIs within both Dol2 and Dol3. The molar volume of these FIs ranges between 18.81 and 19.94 cm^3/mol (*i.e.* density between 0.970 and 0.910 g/cm^3). Trapping conditions for the different FIs were calculated by means of isochores constructed for the *Th* mode value (95°C ± 10°C). Both the minimum and the maximum salinity values (*i.e.* 2 and 6 wt% NaCl eq, respectively) were

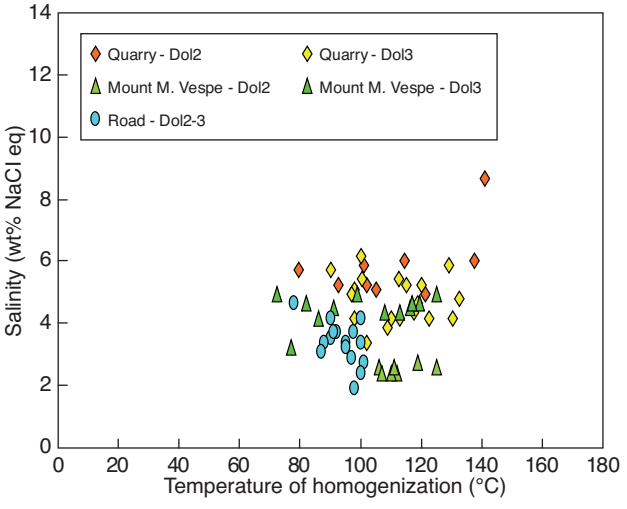

Figure 10

Bivariate plots showing the covariance between *Th* and salinity data. Salinity is expressed in wt% NaCl eq. Slight thermal reequilibration affected the samples in which single FIs assemblages retained consistent data.

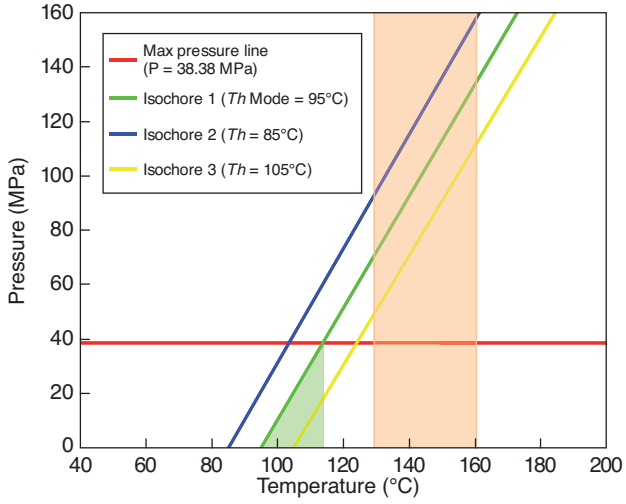

Figure 11

P-T plot illustrating the maximum pressure correction for the *Th* of the dolomite FIs. The isochores were constructed for a fluid with mean salinity of 4.2 wt% NaCl eq. and for three different *Th* (mode value ± 10°C), *i.e.* 95°C (green line), 85°C (blue line) and 105°C (yellow line). A line of constant pressure (in red) was built for the maximum burial conditions (38.38 MPa). The intersection points between this pressure line and the isochores define the maximum *P-T* conditions for FIs trapping. The pinkish square defines the field of temperature (130-160°C) which characterized the peak burial conditions of the first compressional phase. The greenish triangle includes the possible field of temperatures for dolomitization after maximum pressure correction on the *Th* mode value (*i.e.* 95°C).

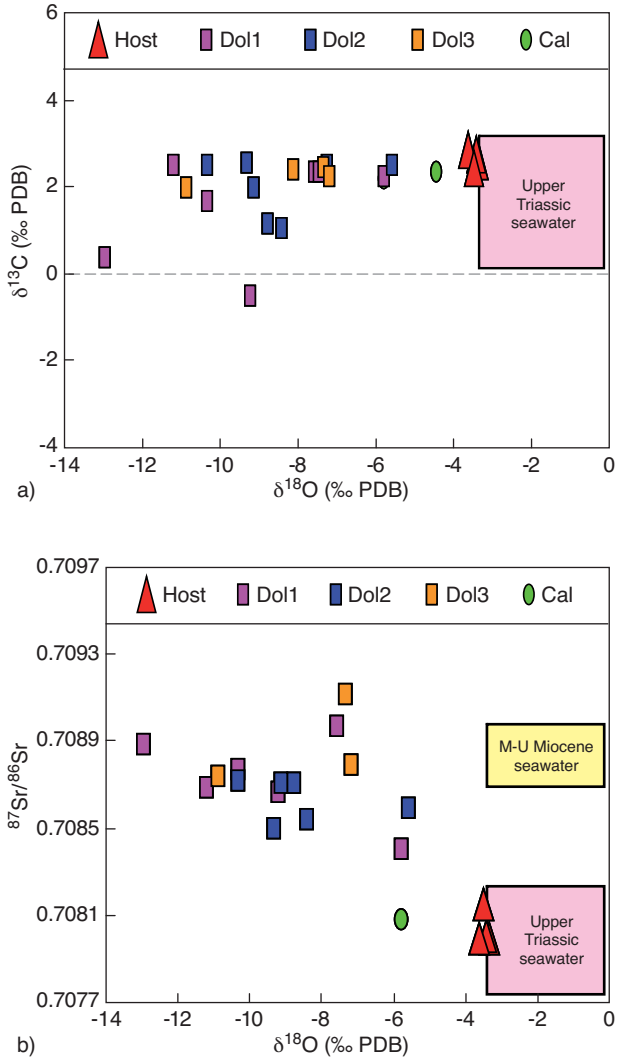

Figure 12

O, C and Sr isotope composition of the different carbonate phases analyzed. The isotope composition of the Upper Triassic seawater (Veizer *et al.*, 1999) is reported in the pink frame. a) Covariation plot between $\delta^{18}O$ and $\delta^{13}C$; b) Covariation plot between $\delta^{18}O$ and $^{87}Sr/^{86}Sr$ ratios. The isotope composition of Middle-Upper Miocene seawater (McArthur *et al.*, 2001) is reported in the yellow frame.

used for this calculation, in order to take into account the changes in isochore slopes induced by salinity variation. Considering the maximum burial of 3.8 km, and peak temperatures of 130-160°C experienced by the studied succession (Corrado *et al.*, 2005; Mazzoli *et al.*, 2008), we may assume that hydrostatic pressure conditions prevailed during dolomitization. According to a hydrostatic pressure gradient of 10.1 MPa/km (obtained by considering a seawater density of 1.03 g/cm^3) the peak burial depth would have corresponded to a maximum pressure of 38.38 MPa. In a *P-T* diagram the intersection points between the constructed isochores and this maximum pressure give the maximum *P-T* condition for dolomite precipitation *(Fig. 11)*. The calculated maximum trapping temperatures for the different salinities are equal to *Th* +15-20°C. True temperature of dolomitization must fall in between.

6 GEOCHEMISTRY AND MINERALOGY

The dolomite stoichiometry calculated for 4 samples of Dol1 and 4 samples of Dol2 give values between 50.3 and 50.9 mol% $CaCO_3$, in agreement with the suspected late burial origin for the dolomites (Lumsden and Chimahusky, 1980). Two samples of Dol3 are slightly non-stoichiometric and show values in the range 51.0 to 51.6 mol% $CaCO_3$, possibly due to the presence of significant Fe in the crystal lattice, also suggested by the common lack of luminescence of this dolomite phase. The O and C stable isotope analyzes performed on the different carbonate phases are summarised in Figure 12a. In Figure 12b the $\delta^{18}O$ values are plotted against the $^{87}Sr/^{86}Sr$ ratios. The precursor limestones from

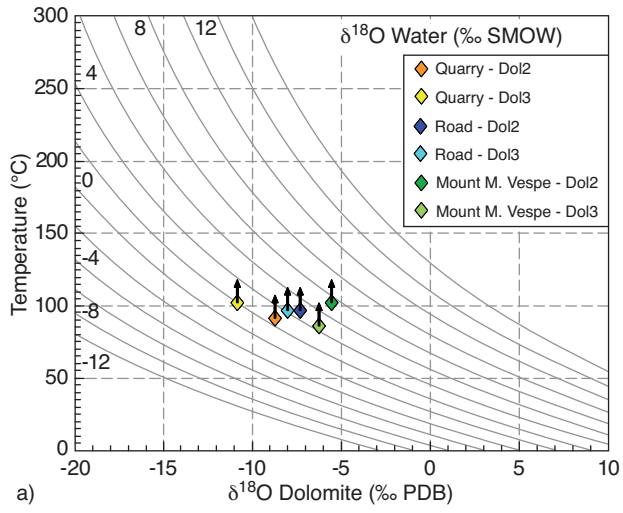

Figure 13

Plot of precipitation temperature versus $\delta^{18}O$ values of Dol2 and Dol3. The $\delta^{18}O$ composition of the fluid in equilibrium with dolomite as function of the temperature was calculated using the fractionation equation of Land (1983). The $\delta^{18}O$ values of single dolomite sample were plotted against the mode values of *Th* for the same sample. Arrows above the dots indicate the maximum possible pressure correction for each sample.

the *Calcari con Selce* Formation have $\delta^{13}C$ and $^{87}Sr/^{86}Sr$ values which overlap those of the Upper Triassic seawater (Veizer *et al*., 1999), whereas the $\delta^{18}O$ values result to be slightly more negative compared to the coeval seawater. These values are the result of slight ^{18}O depletion in the carbonates as a consequence of the temperatures experienced during burial. The blocky calcite, which replaced some of the chert nodules, display $\delta^{18}O$ values within the burial range (Choquette and James, 1990), and Sr isotope ratios in line with Triassic seawater stored as limestones pore water *(Fig. 12 a, b)*.

Samples from the three different dolomite phases (Dol1, Dol2 and Dol3) show $\delta^{13}C$ inherited from the precursor limestones, with only two samples of Dol1 having lower values. By contrast, they show a large spread of $\delta^{18}O$, ranging from – 6 to – 13 per mil PDB, with most of the values falling in the range – 7 to – 11 per mil. Despite such a dispersion in O-isotope data, the three dolomite phases overall display an isotopic trend typical of burial dolomites (Morse and Mackenzie, 1990). This is also confirmed by the Sr-isotope data which indicate a slightly more radiogenic nature of the dolomites compared to the precursor limestones (Veizer *et al*., 1999). No significant geochemical differences nor trends were observed from one dolomite phase to another belonging to the same hand specimen.

The oxygen isotope composition of the fluids responsible for dolomitization can be constrained by combining the results of geochemistry and microthermometry *(Fig. 13)*. The $\delta^{18}O$ values of single dolomite cements were plotted against the mode values of *Th* for the same cement. It results that the fluids responsible for Dol2 and Dol3 precipitation had $\delta^{18}O$ values between 0 and 5 per mil SMOW and most commonly between 1 and 3 per mil. These values could be increased of about 1.5 to 2 per mil by shifting the dots upward of 15-20°C if considering the maximum possible temperatures obtained after pressure correction for peak burial conditions (see arrows in *Fig. 13*).

7 DISCUSSION

The field, petrographic and geochemical characteristics of the investigated dolostone bodies are adequate to describe them as non-planar, saddle, burial, epigenetic or high temperature dolomites (Hewett, 1928; Beales and Jackson, 1966; Radke and Mathis, 1980; Anderson and Macqueen, 1982; Boni *et al*., 2000b; Gasparrini e*t al*., 2006a). All these terms found in literature commonly refer to dolostone bodies consisting of grey to black replacive, coarse dolomite containing variously shaped cavities lined by void-filling, white sparry dolomite.

Generally these rocks are interpreted to be formed from very saline and relatively warm fluids circulating late during the diagenetic evolution of carbonates (Radke and Mathis, 1980; Gasparrini *et al*., 2006b) and are typically associated to MVT mineralizations (Beales and Jackson, 1966; Anderson and Macqueen, 1982). In many instances, these fluids ascend through sub-vertical extensional faults in relatively undeformed, cratonic or foreland sedimentary basin (Davies and Smith, 2006 and references therein). However, several examples have been described in the last years of zebra-dolomites formed in the external units of fold and thrust belts (Qing and Mountjoy, 1994; Boni *et al*., 2000b; Swennen *et al*., 2003; Vandeginste *et al*., 2005; Gasparrini *et al*. 2006a, b). Moreover, it is increasingly clear that the fluid-flow may occur at different moments of the evolution from burial to collision and that even fluids with low salinities may be involved in the dolomitization process (Al-Aasm, 2003; Ronchi *et al*., 2010).

Within this wide *spectrum* of genetic models, the Lagonegro dolostone bodies represent another example of dolomitization occurring within a fold and thrust belt, in the external part of a collisional orogen. The cross-cutting relationships with cleavage and veins formed during the first phase of buckling indicate that the dolomites originated after these tectonic features, *i.e*. after deep burial of the sedimentary basin. Moreover, the local occurrence of zebra-structures showing *en echelon* geometries, suggestive of simple shear deformation, would agree with a syn-deformational genesis.

The origin of some zebra-dolomites as simple shear-related structures has been reported by several authors (Wallace

et al., 1994; Davies and Smith, 2006). The *en echelon* vein arrays observed at Pignola indicate that some shear-deformation was probably effective during replacement. However these features are quite uncommon possibly because they are overprinted by later structures. In fact, the Pignola outcrop bears abundant evidence of a genesis of the zebra-structures mainly as a result of extension and related fracturing of limestone beds in an over-pressured regime. Particularly, the brecciated fabrics *(Fig. 6b)* suggest that they formed by hydraulic fracturing under the action of overpressured fluids. The fluids ingression must have broken the precursor rock into pieces, where dolomite replacement caused the grey dolomite and cementation the white dolomite. Thus, even though some evidences of dissolution are present, we believe that most of the space for the precipitation of the white void-filling phase was created by extension.

The origin of the white, void-filling dolomite bands in an over-pressured rock has been suggested by many authors (Boni *et al*., 2000b; Vandeginste *et al*., 2005; Gasparrini *et al*., 2006a, b; Diehl *et al*., 2010). In an alternative interpretation, Merino *et al*. (2006) have suggested that the white bands represent displacive veins, *i.e*. veins that pushed aside the host dolostone as they grew. According to the latter author, for each white band, a stylolite should form in the adjacent grey band in order to compensate for the volume added by the white veins growth. However in the investigated outcrops, the association of zebra banding with stylolites is by no way systematic, therefore the model of Merino *et al*. (2006) is not favoured.

The position of the *Calcari con Selce* Formation, calcareous and intensely fractured, sandwiched between the fine-clastic *Monte Facito* Formation (below) and the siliceous and fine-clastic Jurassic to Lower Cretaceous formations (*Scisti Silicei* and *Galestri*, above), is particularly favourable for focussing fluid-flow and engendering over-pressure during tectonic shortening. Noteworthy is that overpressures have been actually encountered during well operation in the *mélange* zone which separates the Lagonegro Units and the tectonically underlying Apulian Platform reservoir carbonates (Mazzoli *et al*., 2001; Shiner *et al*., 2004).

The timing of dolomitization may be constrained by referring to available thermometric data from the southern Apennines (Aldega *et al*., 2003, 2005; Corrado *et al*., 2002, 2005; Mazzoli *et al*., 2008). A first phase of buckling and associated reverse faulting took place in the Miocene with the development of slaty cleavage in the pelitic units (Mazzoli *et al*., 2001; Shiner *et al*., 2004) at an approximate depth, in the Val d'Agri area, of 3.8 km and peak temperatures of 130-160°C. A second phase of thrusting coincided with the beginning of exhumation and NNE-directed shortening and led to the tectonic doubling of the Lagonegro Units. This phase is dated 5.5 to 2.5 Ma (Mazzoli *et al*., 2008).

According to the previously calculated maximum trapping temperatures *(see Sect. 5 and Fig. 11)*, even by taking into account the maximum possible trapping conditions, the dolomitizing fluid had temperatures lower than those reached during peak burial in the first deformation stage. Instead, the calculated temperatures fit in with the second phase of deformation, soon after exhumation had started at an approximate temperature of 110-115°C. An upper limit for the timing of dolomitization is provided by apatite fission track data (Corrado *et al*., 2005; Mazzoli *et al*., 2008) which indicate that the succession experienced temperatures of 100-110°C between 5 and 4 Ma under 3-4 km of burial. These calculations are made in the assumption that the dolomitizing fluids were in thermal equilibrium with the host rock. In the studied area, no evidence for a hydrothermal origin can be found, such as relationships of the dolostone bodies with deep-seated normal faults. Nevertheless, with the present knowledge, hydrothermal conditions for the fluids cannot be completely ruled out.

The fluids responsible for dolomitization had a range of salinities close to that of seawater and were slightly more radiogenic than Upper Triassic seawater. The oxygen isotope composition inferred for the dolomitizing fluids *(Fig. 13)* is comprised between values characteristic of seawater and those of saline formation waters, even by taking into account the maximum possible pressure correction for the homogenization temperatures.

Most models of regional fluid-flow in foreland basins assume two main sources: meteoric waters and saline formation waters (Garven and Freeze, 1984; Qing and Mountjoy, 1994; Al-Aasm, 2003). In the Lagonegro Units, the possibility of a massive input of meteoric waters from the already emergent chain is not consistent with geochemical data.

Ronchi *et al*. (2010) compared the geochemistry of fluids for similar case of syntectonic dolomitization in the Southern Alps *versus* central Apennines. They found evidence of mixing of meteoric waters with deep basinal brines in the Alpine belt, whereas in the central Apennines data point to the action of saline formation waters alone. These authors assumed that meteoric recharge would be in agreement with the higher relief of the Alpine belt during collision, that probably caused increasing rainfall and provided the hydraulic head which allowed a deeply penetration of surface waters. By contrast, these factors were absent in central Apennines with consequent absence of meteoric recharge (Ronchi *et al*., 2010). The southern Apennines fold and thrust belt could represent a further case of a low relief belt, lacking a significant meteoric influx in the deep subsurface.

Two possible sources for the dolomitizing fluids of the Lagonegro Units can be envisaged. Fluids could relate to pore waters squeezed out from the surrounding Triassic and Cretaceous fine-clastic formations (*Monte Facito* and *Galestri*, respectively). In this case, however, because of the prolonged water-rock interaction in the subsurface, more radiogenic and more saline fluids would be expected compared to the low salinity and only slightly radiogenic fluids

inferred from the present study data. The other probable fluid source could be represented by marine formation waters expelled from the Miocene formations involved in the *mélange*. It is significant, in this respect, that Sr isotope values reported for the studied dolomites are close to those of Middle-Upper Miocene seawater (see *Fig. 12b*; McArthur *et al*., 2001). These two scenarios should be taken as working hypotheses, to be tested after a larger data set is collected and a quantitative approach is attempted.

According to the available regional geology literature, dolostones within the *Calcari con Selce* Formation occur only in the northern area of the Lagonegro Basin *(Fig. 1)*. Here, the Lagonegro Units consist of two main thrust sheets, the dolomite being restricted to the upper one (Scandone, 1967). A reasonable explanation for this distribution could be that the fluid-flow may have been focussed up-dip by the geometry of the thrust surfaces. Nevertheless, it must be pointed out that the outcrops from the southern area, which lack dolostone occurrences, suffered a deeper burial (Mazzoli *et al*., 2008). A possible scenario to explain this regional dolostone distribution should take into account the different exhumation timing between the northern and southern parts of the Lagonegro Basin.

The wide distribution of dolostone bodies in the Lagonegro Units, as reported in the literature (Scandone, 1967), suggests that the fluid-flow leading to dolomitization was a major phenomenon affecting the fold and thrust belt. Based on the examples from north America (Betkhe and Marshak, 1990; Leach *et al*., 2001; Gregg, 2004), this kind of massive fluid-flow within the fold and thrust belt could have reached also the foreland. In the southern Apennines, the foreland of the Miocene fold and thrust belt was represented by shallow-water carbonates of the Apulian Platform. These were subsequently buried beneath the nappe stack, during late deformation stages, providing the structural traps hosting major oil fields (Casero *et al*., 1991; Mattavelli *et al*., 1993; Sciamanna *et al*., 2004; Shiner *et al*., 2004). Thus, it could be expected that the dolostone bodies which are reported in the Apulian subsurface (Murgia *et al*., 2004) might have the same origin, this giving economic significance to the fluid-flow that took place along with the southern Apennines belt formation.

CONCLUSIONS

The Triassic pelagic carbonates of the Lagonegro Units from the southern Apennines fold and thrust belt host discordant dolostone bodies showing fabric and petrographic characteristics typical of late burial saddle dolomites displaying zebra-like structures. Field evidences indicate that the rock fabric was controlled by regular bedding of the micritic, pelagic limestones; it was the result of replacement and void-filling precipitation in an environment characterized by high pore fluid pressure. The geochemistry of the dolomite samples indicates an origin by warm fluids (110-115°C) with a salinity close to that of seawater and O-isotope composition comprised between seawater and formation waters. Integration with available thermal data into the regional deformation history by assuming a fluid in thermal equilibrium with the host rocks suggests that the fluid-flow took place after maximum burial, in the early stages of exhumation, between 5 and 4 Ma and under 3-4 km of burial. The location of the dolomitized *Calcari con Selce* Formation between relatively impermeable clastic formations was instrumental to the focussing of over-pressured fluids.

It is suggested that dolomitization was accomplished by squeezing out of formation waters from the surrounding clastic formations, or from Miocene marine pore-waters from the deeper *mélange* units.

According to regional geology literature, the dolomitization was a widespread event. This major fluid influx is associated with the development of the Neogene fold and thrust belt. It could be argued that dolomitization may have affected also the Apulian Platform carbonates located in the foreland. The latter, now buried below the nappe stack, host the major oil fields of continental Europe. A complete regional and geochemical study, presently in progress, will allow a better understanding of the factors controlling the dolomitization process, also providing some clues for exploration in this complex petroleum system.

REFERENCES

Al-Aasm I. (2003) Origin and characterization of hydrothermal dolomite in the Western Canada Sedimentary Basin, *J. Geochem. Explor*. **78-79**, 9-15.

Aldega L., Cello G., Corrado S., Cuadros J., Di Leo P., Giampaolo C., Invernizzi C., Martino C., Mazzoli S., Schiattarella M., Zattin M., Zuffa G. (2003) Tectono-sedimentary evolution of the Southern Apennines (Italy): thermal constraints and modelling, *Atti Ticinensi di Scienze della Terra - Ser. Spec*. **9**, 135-140.

Aldega L., Corrado S., Di Leo P., Giampaolo C., Invernizzi C., Martino C., Mazzoli S., Schiattarella M., Zattin M. (2005) The Southern Apennines case history: thermal constraints and reconstruction of tectonic and sedimentary burials, *Atti Ticinensi di Scienze della Terra* **10**, 45-53.

Anderson G.M., Macqueen R.W. (1982) Ore deposit models - 6. Mississippi Valley-type lead zinc deposits, *Geosci. Can*. **9**, 108-117.

Arne D.C., Kissin S.A. (1989) The significance of "diagenetic crystallization rhythmites" at the Nanisivik Pb-Zn-Ag deposit, Baffin Island, Canada, *Mineralium Deposita* **24**, 230-232.

Bakker R.J. (2003) Package FLUIDS 1. Computer programs for analysis of fluid inclusion data and for modelling bulk fluid properties, *Chem. Geol*. **194**, 3-23.

Bakker R.J. (2009) Package FLUIDS. Part 3: Correlations between equation of state thermodynamics and fluid inclusions, *Geofluids* **9**, 3-23.

Beales F.W., Hardy J.L. (1980) Criteria for the recognition of diverse dolomite types with an emphasis on studies on host rocks for Mississippi Valley-Type ore deposits, *Soc. Econ. Petrol. Min. Spec. Publ*. **28**, 197-213.

Beales F.W., Jackson S.A. (1966) Precipitation of lead-zinc ores in carbonate reservoirs as illustrated by Pine Point ore field, Canada, *T. I. Min. Metall. B* **75**, 278-285.

Berger Z., Davies G.R. (1999) The development of linear hydrothermal dolomite (HTD) reservoir facies along wrench or strike slip fault systems in the Western Canada Sedimentary Basin, *Reservoir* **26**, 1, 34-38.

Bethke C.M., Marshak S. (1990) Brine migrations across North America – The plate tectonics of groundwater, *Annu. Rev. Earth Planet. Sci.* **18**, 287-315.

Bodnar R.J. (1993) Revised equation and table for determining the freezing point depression of H_2O-NaCl solutions, *Geochim. Cosmochim. Acta* **57**, 683-684.

Bodnar R.J., Vityk M.O. (1994) Interpretation of microthermometric data for H_2O-NaCl fluid inclusions, in *Fluid inclusions in minerals: methods and applications*, De Vivo B., Frezzotti M.L. (eds), Virginia Tech, Potignano-Siena, pp. 117-130.

Boni M., Iannace A., Bechstädt T., Gasparrini M. (2000a) Hydrothermal dolomites in SW Sardinia (Italy) and Cantabria (NW Spain): evidence for late- to post-Variscan widespread fluid-flow events, *J. Geochem. Explor.* **69-70**, 225-228.

Boni M., Parente G., Bechstädt T., De Vivo B., Iannace A. (2000b) Hydrothermal dolomites in SW Sardinia (Italy): evidence for a widespread late-Variscan fluid flow event, *Sediment. Geol.* **131**, 181-200.

Casero P., Roure F., Endignoux L., Moretti I., Müller C., Sage L., Vially R. (1988) Neogene geodynamic evolution of the Southern Apennines, *Memorie della Società Geologica Italiana* **41**, 109-120.

Casero P., Roure F., Vially R. (1991) Tectonic framework and petroleum potential of southern Apennines, in *Generation, accumulation and production of Europe's hydrocarbon*, Spencer M. (ed.), EAPG Spec. Pub. **1**, 381-387.

Cello G., Mazzoli S. (1998) Apennine tectonics in southern Italy: A review, *J. Geodynamics* **27**, 2, 191-211.

Choquette P.W., James N.P. (1990) Limestones – the burial diagenetic environment, in *Diagenesis. Geoscience Canada Reprint Series 4*, McIlearth I.A., Morrow D.W. (eds), Ottawa, pp. 75-111.

Ciarapica G., Cirilli S., Panzanelli Fratoni R., Passeri L., Zaninetti L. (1990) The Monte Facito Formation (Southern Apennines), *Bollettino della Società Geologica Italiana* **109**, 1, 135-142.

Corrado S., Invernizzi C., Mazzoli S. (2002) Tectonic burial and exhumation in a foreland fold and thrust belt: The Monte Alpi case history (Southern Apennines, Italy), *Geodinamica Acta* **15**, 3, 159-177.

Corrado S., Aldega L., Di Leo P., Giampaolo C., Invernizzi C., Mazzoli S., Zattin M. (2005) Thermal maturity of the axial zone of the southern Apennines fold-and-thrust belt (Italy) from multiple organic and inorganic indicators, *Terra Nova* **17**, 56-65.

Davies G.R., Smith L.B.J. (2006) Structurally controlled hydrotermal dolomite reservoir facies: An overview, *AAPG Bull.* **90**, 11, 1641-1690.

Deming D., Nunn J.A. (1991) Numerical simulations of brine migration by topography-driven recharge, *J. Geophys. Res.* **96**, 2485-2499.

Diehl S.F., Hofstra A.H., Koenig A.E., Emsbo P., Christiansen W., Johnson C. (2010) Hydrothermal Zebra Dolomite in the Great Basin, Nevada – Attributes and Relation to Paleozoic Stratigraphy, Tectonics, and Ore Deposits, *Geosphere* **6**, 5, 663-690.

Fontboté L., Amstutz G.C. (1983) Facies and sequence analysis of diagenetic crystallization rhythmites in strata-bound Pb-Zn (Ba-F) deposits in the Triassic of central and southern Europe, in *Mineral deposits of the Alps and of the Alpine epoch in Europe*, Schneider H.J. (ed.), Springer, Berlin Heidelberg New York, pp. 347- 358.

Garven G. (1985) The role of regional fluid flow in the genesis of the Pine Point deposit, Western Canada sedimentary basin, *Econ. Geol.* **80**, 307-324.

Garven G., Freeze R. (1984) Theoretical analysis of the role of groundwater flow in the genesis of stratabound ore deposits, *Am. J. Sci.* **284**, 1085-1174.

Gasparrini M., Bakker R.J., Bechstädt T. (2006a) Characterisation of dolomitising fluids in the Carboniferous of the Cantabrian Zone (NW Spain): a fluid inclusion study with cryo-Raman spectroscopy, *J. Sediment. Res.* **76**, 1304-1322.

Gasparrini M., Bechstädt T., Boni M. (2006b) Massive hydrothermal dolomite in the southwestern Cantabrian Zone (Spain) and its relation to the late Variscan evolution, *Mar. Petrol. Geol.* **23**, 543-568.

Ge S., Garven G. (1994) A theoretical model for thrust-induced deep groundwater expulsion with application to the Canadian Rocky Mountains, *J. Geophys. Res.* **99**, 13851-13868.

Goldstein R.H., Reynolds T.J. (1994) *Systematics of fluid inclusions in diagenetic minerals. SEPM Short Course 31*, SEPM (eds), Tulsa, Oklahoma.

Gregg J.M. (2004) Basin fluid flow, base-metal sulphide mineralization and the development of dolomite petroleum reservoirs, in *The Geometry and Petrogenesis of Dolomite Hydrocarbon Reservoirs*, Braithwaite C.J.R., Rizzi G., Darke G. (eds), *Geol. Soc. London Spec. Publ.* **235**, 157-175.

Hewett D.F. (1928) Dolomitization and ore deposition, *Econ. Geol.* **23**, 821-863.

Hurley N.F., Budros R. (1990) Albion-Scipio and Stoney Point fields, U.S.A., Michigan Basin, in *Stratigraphic Traps I: AAPG Treatise of Petroleum Geology, Atlas of Oil and Gas Fields*, Beaumont E.A., Foster N.H. (eds), Tulsa, pp. 1-37.

Jackson S.A., Beales F.W. (1967) An aspect of sedimentary basin evolution: the concentration of Mississippi Valley-type ores during late stages of diagenesis, *Bull. Can. Pet. Geol.* **15**, 383-433.

Krumgalz B.S., Pogorelsky R., Pitzer K.S. (1996) Volumetric properties of single aqueous electrolytes from zero to saturation concentrations at 298.15 K represented by Pitzer´s Ion-Interaction Equation, *J. Phys. Chem. Ref. Data* **25**, 663-689.

Land L.S. (1983) The application of stable isotopes to studies of the origin of dolomite and to problems of diagenesis of clastic sediments, in *Stable isotopes in sedimentary geology*, Arthur M.A., Anderson T.F., Kaplan I.R., Veizer J., Land L.S. (eds), *SEPM Short Course* **10**, 4.1-4.22.

Lavoie D., Chi G. (2010) Lower Paleozoic foreland basins in eastern Canada: tectono-thermal events recorded by faults, fluids and hydrothermal dolomites, *Bull. Can. Pet. Geol.* **58**, 1, 17-35.

Leach D.L., Bradley O., Lewchuk M.T., Symons D.T.A., Marsily G.D., Brannon J. (2001) Mississippi Valley-type lead-zinc deposits through geological time: implications from recent age-dating research, *Mineralium Deposita* **36**, 711-740.

Lumsden D.N., Chimahusky J.S. (1980) Relationship between dolomite nonstoichiometry and carbonate facies parameters, in *Concepts and models of dolomitization*, Zenger D.H., Dunham, J.B., Ethington R.L. (eds), *SEPM Special Publication* **28**, 87-110.

Machel H.G., Cavell E.A., Patey K.S. (1996) Isotopic evidence for carbonate cementation and recrystallization, and for tectonic expulsion of fluids into the Western Canada Sedimentary Basin, *Geol. Soc. Am. Bull.* **108**, 1108-1119.

Machel H.G. (2004) Concepts and models of dolomitization: a critical reappraisal, in *The Geometry and Petrogenesis of Dolomite Hydrocarbon Reservoirs*, Braithwaite C.J.R., Rizzi G., Darke G. (eds), *Geol. Soc. London Spec. Publ.* **235**, 7-63.

Mattavelli L., Pieri M., Groppi G. (1993) Petroleum exploration in Italy: a review, *Mar. Petrol. Geol.* **10**, 410-425.

Mazzoli S., Di Bucci D. (2003) Critical displacement for normal fault nucleation from en-échelon vein arrays in limestones: A case study from the southern Apennines (Italy), *J. Struct. Geol.* **25**, 7, 1011-1020.

Mazzoli S., Helman M. (1994) Neogene patterns of relative plate motion for Africa–Europe: some implications for recent central Mediterranean tectonics, *Geol. Rundschau* **83**, 464-468.

Mazzoli S., Barkham S., Cello G., Gambini R., Mattioni L., Shiner P., Tondi E. (2001) Reconstruction of continental margin architecture deformed by the contraction of the Lagonegro basin, Southern Apennines, Italy, *J. Geol. Soc.* **158**, 2, 309-320.

Mazzoli S., Invernizzi C., Marchegiani L., Mattioni L., Cello G. (2004) Brittle-ductile shear zone evolution and fault initiation in limestones, Monte Cugnone (Lucania), southern Apennines, Italy, *Geol. Soc. London Spec. Publ.* **224**, 353-373.

Mazzoli S., D'Errico M., Adelga L., Corrado S., Invernizzi C., Shiner P., Zattin M. (2008) Tectonic burial and "young" (<10 Ma) exhumation in the southern Apennines fold-and-thrust belt (Italy), *Geology* **36**, 3, 243-246.

McArthur J.M., Howarth R.J., Bailey T.R. (2001) Strontium isotope stratigraphy: LOWESS Version 3. Best-fit line to the marine Sr-isotope curve for 0 to 509 Ma and accompanying look-up table for deriving numerical age, *J. Geol.* **109**, 155-169.

Merino E., Canals A., Fletcher R.C. (2006) Genesis of self-organized zebra textures in burial dolomites: Displacive veins, induced stress, and dolomitization, *Geologica Acta* **4**, 3, 383-393.

Morrow D. (1998) Regional subsurface dolomitization: models and constraints, *Geosci. Can.* **25**, 2, 57-70.

Morse J.M., MacKenzie F.T. (1990) Carbonates as sedimentary rocks in subsurfaces process, in *Geochemistry of sedimentary carbonates*, Elsevier, Amsterdam.

Mostardini F., Merlini S. (1986) Appennino centro-meridionale: sezioni geologiche e proposta di modello strutturale, *Memorie della Società Geologica Italiana* **35**, 177-202.

Murgia M.V., Ronchi P., Ceriani A. (2004) Dolomitization processes and their relationships with the evolution of an orogenic belt (Central Apennines and peri-adriatic foreland, Italy), in *Deformation, Fluid Flow, and Reservoir Appraisal in Foreland Fold and Thrust Belts*, Swennen R., Roure F., Granath J.W. (eds), AAPG Hedberg Series 1, Tulsa, Oklahoma, USA, pp. 277-294.

Nielsen P., Swennen R., Muchez P.H. Keppens R. (1998) Origin of the Dinantian zebra dolomites south of the Brabant-Wales Massif, Belgium, *Sedimentology* **45**, 727-743.

Oliver J. (1986) Fluids expelled tectonically from orogenic belts: their role in hydrocarbon migration and other geologic phenomena, *Geology* **14**, 99-102.

Qing H., Mountjoy E.W. (1994) Formation of coarse-crystalline, hydrothermal dolomite reservoirs in the Presqu'ile Barrier, Western Canada Sedimentary Basin, *AAPG Bull.* **78**, 55-77.

Radke B.M., Mathis R.L. (1980) On the formation and occurrence of saddle dolomite, *J. Sediment. Petrol.* **50**, 1149-1168.

Ronchi P., Di Giulio A., Ceriani A., Scotti P. (2010) Contrasting fluid events giving rise to apparently similar diagenetic products; late-stage dolomite cements from the Southern Alps and central Apennines, Italy, *Geol. Soc. London Spec. Publ.* **329**, 397-413.

Rosenbaum J., Sheppard S.M. (1986) An isotopic study of siderites, dolomites and ankerites at high temperatures, *Geochim. Cosmochim. Acta* **50**, 1147-1150.

Scandone P. (1967) Studi di geologia lucana: la serie calcareo-silico-marnosa e i suoi rapporti con l'Appennino calcareo, *Bollettino Società dei Naturalisti in Napoli* **76**, 1-175.

Scandone P. (1972) Studi di geologia lucana: carta dei terreni della serie calcareo-silico-marnosa e note illustrative, *Bollettino Società dei Naturalisti in Napoli* **81**, 225-300.

Sciamanna S., Sassi W., Rudkiewicz J.L., Gambini R., Mosca F. (2004) Predicting Hydrocarbon Generation and Expulsion in the Southern Apennines Thrust Belt by 2-D Integrated Structural and Geochemical Modeling: Part I: Structural and thermal Evolution, in *Deformation, Fluid Flow, and Reservoir Appraisal in Foreland Fold and Thrust Belts*, Swennen R., Roure F., Granath J.W. (eds), AAPG Hedberg Series 1, Tulsa, Oklahoma, USA, pp. 51-67.

Shah M., Nader F.H., Dewit J., Swennen R., Garcia D. (2010) Fault-related hydrothermal dolomites in Cretaceous carbonates (Cantabria, northern Spain): Results of petrographic, geochemical and petrophysical studies, *Bull. Soc. Géol. Fr.* **181**, 4, 391-407.

Shiner P., Beccacini A., Mazzoli S. (2004) Thin-skinned *versus* thick-skinned structural models for Apulian carbonate reservoirs: Constraints from the Val D'Agri Fields, *Mar. Petrol. Geol.* **21**, 805-827.

Swennen R., Ferket H., Benchilla L., Roure F., Ellam R. (2003) Fluid flow and diagenesis in carbonate dominated Foreland Fold and Thrust Belts: petrographic inferences from field studies of late-diagenetic fabrics from Albania, Belgium, Canada, Mexico and Pakistan, *J. Geochem. Explor.* **78-79**, 481-485.

Taylor T.R., Sibley D.F. (1986) Petrographic and geochemical characteristics of dolomite in the Trenton Formation, Ordovician, Michigan Basin, *Sedimentology* **33**, 61-86.

Turpin M., Kohler E., Nader F.H. (2012) Stoichiometric characterization of dolomites by Cell and Rietveld Refinements (Middle Triassic, French Jura): A new approach, *Oil Gas Sci. Technol.* **67**, 1, 77-95.

Vandeginste V., Swennen R., Gleeson S.A., Ellam R.M., Osadetz K., Roure F. (2005) Zebra dolomitization as a result of focused fluid flow in the Rocky Mountains Fold and Thrust Belt, Canada, *Sedimentology* **52**, 1067-1095.

Veizer J., Ala D., Azmy K., Bruckschen P., Buhl D., Bruhn F., Carden G.A.F., Diener A., Ebneth S., Godderis Y., Jasper T., Korte C., Pawellek F., Podlaha O.G., Strauss H. (1999) $^{87}Sr/^{86}Sr$, $\delta^{13}C$ and $\delta^{18}O$ evolution of Phanerozoic seawater, *Chem. Geol.* **161**, 59-88.

Wallace M.W., Both R.A., Ruano S.M., Hach-Ali P.F., Lees T. (1994) Zebra textures from carbonate-hosted sulfide deposits: Sheet cavity networks produced by fracture and solution enlargement, *Econ. Geol.* **89**, 1183-1191.

Warren J. (2000) Dolomite: occurrence, evolution and economically important association, *Earth-Sci. Rev.* **52**, 1-81.

Wendte J., Al-Aasm I., Chi G., Sargent, D. (2009) Fault/fracture controlled hydrothermal dolomitization and associated diagenesis of the Upper Devonian Jean Marie Member (Redknife Formation) in the July Lake area of northeastern British Columbia, *Bull. Can. Pet. Geol.* **57**, 3, 275-322.

Final manuscript received in May 2011
Published online in February 2012